Weighted Sum-Rate Maximization for MIMO Downlink Systems Powered by Renewables

Shuyan Hu, Yu Zhang, *Member, IEEE*, Xin Wang, *Senior Member, IEEE*, and Georgios B. Giannakis, *Fellow, IEEE*

***Abstract*— Optimal resource management for smart grid powered multi-input multi-output (MIMO) systems is of great importance for future green wireless communications. A novel framework is put forth to account for the stochastic renewable energy sources (RES), dynamic energy prices, as well as random wireless channels. Based on practical models, the resource allocation task is formulated as an optimization problem that aims at maximizing the weighted sum-rate of the MIMO broadcast channels. A two-way transaction mechanism and storage units are introduced to accommodate the RES variability. In addition to system operating constraints, a budget threshold is imposed on the worst-case energy transaction cost due to the possibly adversarial nature. Capitalizing on the uplink–downlink duality and the Lagrangian relaxation-based subgradient method, an efficient algorithm is developed to obtain the optimal strategy. Generalizations to the setups of time-varying channels and ON–OFF transmissions are also discussed. Numerical results are provided to corroborate the merits of the novel approaches.**

***Index Terms*— Robust energy allocation, uplink-downlink duality, smart grids, weighted sum-rate, Lagrangian relaxation.**

I. Introduction

DOWNLINKS from a base station (BS) to mobile end users are typically modeled as Gaussian broadcast channels (BCs) whose information-theoretic capacity has been well documented; see e.g., [1]–[3]. The capacity-achieving rate and optimal power allocation schemes have been thoroughly investigated for both single-input single-output (SISO) and multi-input multi-output (MIMO) systems. The common anchor point in most existing studies is the assumption that BSs are persistently powered by the conventional power grid. However, the current power network infrastructure is migrating from the aging grid to a "smart" one. The future smart grid has many appealing features and advanced capabilities including e.g., renewable energy sources (RES), two-way energy trading, dynamic pricing based demand-side management, as well as decentralized control [4]–[7].

Integration of smart-grid capabilities into wireless communication systems is arguably one of the most crucial factors to reduce carbon footprint, as well as exploit the full potential of future cellular networks. Towards this goal, [8]–[11] developed optimal resource allocation schemes that maximize the sum-rate for RES-harvesting BCs, where perfect knowledge of the amount of the harvested energy per time slot is assumed to be available *a priori*. Adopting simplified system models with a limited smart-grid capability, a few works dealt with energy-efficient resource allocation for coordinated downlink transmissions; see e.g., [12]–[18]. When the amounts of the harvested energy are known in advance, a recent work [19] investigated the optimal energy exchange strategy among base stations that minimize the energy cost by the cellular network operator through the dynamic pricing based two-way energy trading in a smart grid environment. Building on practical smart-grid models for a green coordinated multi-point (CoMP) system, our recent work [20] developed robust energy management and transmit-beamforming designs that minimize the worst-case energy transaction cost with a guaranteed quality-of-service (QoS). However, existing works have not considered the impact of advanced smart-grid capabilities on the achievable rates of the BCs.

Motivated by the data applications in 4G/5G networks, there has been a growing interest in system designs that aim to maximize the total throughput of the downlink channel for a given power budget. To this end, this paper deals with optimal resource allocation tasks for smart-grid powered MIMO BCs. Equipped with local RES and energy storage units, the BS can perform two-way energy trading with the main grid based on a *dynamic pricing* mechanism. To account for the intermittent and stochastic nature of the RES, we assume that the actual harvested energy amounts are unknown a priori, yet lie in specified uncertainty regions. Capitalizing on practical models,

Manuscript received November 3, 2015; revised March 8, 2016; accepted April 30, 2016. Date of publication May 5, 2016; date of current version August 10, 2016. This work was supported in part by the China Recruitment Program of Global Young Experts, in part by the Program for New Century Excellent Talents in University, in part by the Innovation Program of Shanghai Municipal Education Commission, and in part by the U.S. National Science Foundation under Grant ECCS-1509005, Grant ECCS-1508993, Grant CCF-1423316, Grant CCF-1442686, Grant ECCS-1202135, and Grant ECCS-1509040. This paper was presented at the 7th International Conference on Wireless Communications and Signal Processing, Nanjing, China, October 15-17, 2015. The associate editor coordinating the review of this paper and approving it for publication was L. Dai.

S. Hu is with the Key Laboratory for Information Science of Electromagnetic Waves Ministry of Education, Department of Communication Science and Engineering, Fudan University, Shanghai 200438, China (e-mail: syhu14@fudan.edu.cn).

Y. Zhang is with the Department of Industrial Engineering and Operations Research, University of California, Berkeley, Berkeley, CA 94720 USA (e-mail: yuzhang49@berkeley.edu).

X. Wang is with the Key Laboratory for Information Science of Electromagnetic Waves Ministry of Education, Department of Communication Science and Engineering, Fudan University, Shanghai 200438, China, and also with the Department of Computer and Electrical Engineering and Computer Science, Florida Atlantic University, Boca Raton, FL 33431 USA (e-mail: xwang11@fudan.edu.cn).

G. B. Giannakis is with the Digital Technology Center, Department of Electrical and Computer Engineering, University of Minnesota, Minneapolis, MN 55455 USA (e-mail: georgios@umn.edu).

Color versions of one or more of the figures in this paper are available online at http://ieeexplore.ieee.org.

Digital Object Identifier 10.1109/TWC.2016.2563420

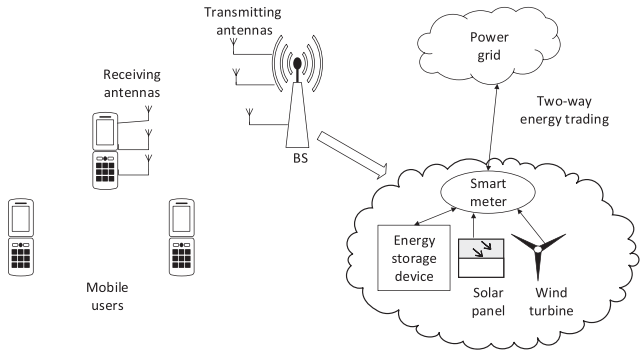

Fig. 1. A smart-grid connected MIMO downlink system.

the task of interest is formulated as a nested optimization problem with a goal of maximizing the achievable sum-rates of the MIMO BCs. A two-way energy trading between the BS and the main grid is introduced as a recourse action to compensate the variability of RES. Besides standard operating constraints, a budget constraint is imposed on the worst-case transaction cost. The original hard problem is reformulated as a convex one leveraging the information-theoretic uplink-downlink duality [11]. The Lagrangian dual based subgradient solver along with a proximal bundle approach is developed to obtain the optimal policy with guaranteed convergence at low complexity. The proposed framework and approaches are further generalized to the scenarios of time-varying MIMO BC and on-off transmissions, where models are more practical and merits of the proposed system are more significant.

The rest of the paper is organized as follows. System models are described in Section II. The problem formulation and proposed approaches are presented in Section III. Generalizations to other scenarios are given in Section IV. Numerical results are provided in Section V, followed by concluding remarks in Section VI.

Notation: Boldface lower (upper) case letters are vectors (matrices); $\mathbb{C}^{M\times N}$ represents the space of $M \times N$ complex matrices; $(\cdot)'$ denotes transpose while $(\cdot)^\dagger$ conjugate transpose; $\mathrm{tr}(\mathbf{A})$ and $|\mathbf{A}|$ represent the trace and determinant of $\mathbf{A}$, respectively; and $\mathbf{A} \succeq \mathbf{0}$ means that $\mathbf{A}$ is positive semi-definite.

II. Modeling Preliminaries

Consider a MIMO downlink system where a BS serves a total of K mobile users; see Fig. 1. The BS is equipped with N_t transmitting antennas while each of the K users has N_r receiving antennas. Different from [8]–[11] where the BS is purely powered by harvesting the RES, here we assume that the BS is jointly supplied by the persistent power sources (e.g., fuel and coal) from the main grid as well as the harvested renewable energy (e.g., solar and wind). Specifically, connected to the main grid via two-way energy trading, the BS is further supported by one or more local energy harvesting facilities (e.g., solar panels and/or wind turbines). Moreover, the BS is equipped with a local storage unit (e.g., flywheel or lithium-ion battery bank) so that it does not have to consume or sell all the harvested energy on the spot, but can save it for later use.

The BS is aware of the downlink channel state information using effective channel estimation, e.g., via limited route feedback. The energy transaction information including the buying and selling prices can be collected by the BS with installed smart meters. The BS controller is in charge of coordinating the energy trading and communications for optimal resource management.

We assume that the slot length of the wireless transmissions is large enough to accommodate the Shannon capacity-achieving encoding schemes. Consider a finite scheduling horizon $\mathcal{T} := \{1, \ldots, T\}$ with a normalized slot duration, unless otherwise specified. Hence, the terms "energy" and "power" will be interchangeably used in Section III.

A. MIMO Broadcasting Model

Let $\mathbf{H}_k \in \mathbb{C}^{N_r\times N_t}$ denote the invariant (over T slots) channel coefficient matrix from the BS to user k for $k = 1, \ldots, K$. Generalization to time-varying channels will be discussed in Section IV. Per slot t, let $\mathbf{x}(t) = \sum_{k=1}^K \mathbf{x}_k(t) \in \mathbb{C}^{N_t}$ denote the transmitted signal vector, which is a superposition of all individual signals intended for the corresponding users. The received complex-baseband signal at user k is thus

$$\boldsymbol{y}_k(t) = \mathbf{H}_k \boldsymbol{x}(t) + \boldsymbol{z}_k(t) \tag{1}$$

where $\boldsymbol{z}_k(t)$ denotes additive complex-Gaussian noise with zero mean and identity covariance matrix $\mathbf{I}$.

It is well known that the MIMO BC capacity can be achieved by dirty paper coding (DPC), where each user perceives no interference from previous encoded users via sequential encoding [21]. With the DPC codeword $\mathbf{x}_k(t)$, the transmit covariance matrix of user k is $\Gamma_{k,t} := \mathbb{E}[\boldsymbol{x}_k(t)\boldsymbol{x}_k^\dagger(t)]$. It is required $\sum_{k=1}^K \mathrm{tr}(\mathbf{\Gamma}_{k,t}) \le P_{x,t}$, where $P_{x,t}$ is the budget of the transmitting power in slot t. Letting $\mathcal{H} := \{\mathbf{H}_1, \ldots, \mathbf{H}_K\}$ collect all downlink channels, the BC capacity region per slot t is then given by

$$\mathcal{C}_{\mathrm{BC}}(P_{x,t}; \mathcal{H}) = \mathrm{Co}\left(\bigcup_{\pi} \mathcal{R}_{\pi}(P_{x,t}; \mathcal{H})\right) \tag{2}$$

where $\mathrm{Co}(\cdot)$ denotes the convex hull; the union is over all permutations π of $\{1, 2, \ldots, K\}$; and

$$\mathcal{R}_{\pi}(P_{x,t}; \mathcal{H}) = \bigcup_{\{\Gamma_{k,t}:\, \sum_{k=1}^K \mathrm{tr}(\Gamma_{k,t}) \le P_{x,t}\}} \left\{ (r_1, \ldots, r_K) : r_{\pi(k)} \le \log \frac{\left|\mathbf{I} + \sum_{u=1}^k \mathbf{H}_{\pi(u)} \Gamma_{\pi(u),t} \mathbf{H}_{\pi(u)}^\dagger\right|}{\left|\mathbf{I} + \sum_{u=1}^{k-1} \mathbf{H}_{\pi(u)} \Gamma_{\pi(u),t} \mathbf{H}_{\pi(u)}^\dagger\right|},\ \forall k \right\}$$

where r_k is the achievable transmission rate of user k.

B. RES Harvesting Model

Let E_t denote the energy harvested during the slot $t-1$, which is available at the beginning of slot t. Different from [11] where the amount of harvested energy per time slot is accurately known a-priori, we assume that $\mathbf{e} := [E_1, \ldots, E_T]'$ is unknown due to the inherently uncertain nature of RES. However, it is assumed that it

lies in an uncertainty set $\mathcal{E}$, which can be obtained by appropriate inference schemes using historical measurements. Two practical paradigms for $\mathcal{E}$ are considered here.

i) The first model amounts to a polyhedral set:

$$\mathcal{E}^{\mathrm{p}} := \Big\{ \boldsymbol{e} \mid \underline{E}_t \le E_t \le \overline{E}_t, \quad E_s^{\min} \le \sum_{t\in\mathcal{T}_s} E_t \le E_s^{\max},\ \mathcal{T} = \bigcup_{s=1}^{S} \mathcal{T}_s \Big\} \tag{3}$$

where $\underline{E}_t$ ($\overline{E}_t$) denotes the lower (upper) bound on E_t; time horizon $\mathcal{T}$ is partitioned into consecutive but non-overlapping sub-horizons $\mathcal{T}_s$, $s = 1, \ldots, S$; while the aggregated energy harvested over the sth sub-horizon is bounded between $E_s^{\min}$ and $E_s^{\max}$.

ii) The second model relies on an ellipsoidal uncertainty set:

$$\mathcal{E}^{\mathrm{e}} := \big\{ \boldsymbol{e} = \hat{\mathbf{e}} + \boldsymbol{\varsigma} \mid \boldsymbol{\varsigma}' \boldsymbol{\Sigma} \boldsymbol{\varsigma} \le 1 \big\} \tag{4}$$

where $\hat{\mathbf{e}} := [\hat{E}_1, \ldots, \hat{E}_T]'$ denotes the nominal energy harvested at the BS, which can be the forecasted energy, or simply its expected value. Vector $\boldsymbol{\varsigma}$ is the forecasting error. The known matrix $\boldsymbol{\Sigma} \succ \mathbf{0}$ quantifies the shape of $\mathcal{E}^{\mathrm{e}}$, and hence determines the quality of forecasting.

Remark 1 (Applicability of RES Models): The uncertainty sets are postulated to capture the realizations of the uncertain renewable generations. With the goal of including as many as possible uncertain realizations, an uncertainty set can be in an arbitrary shape in general. Featuring the information of the first and second order statistics of the random quantities, polyhedral or ellipsoidal sets are the most common choices [22]. These two types of sets are readily to obtain from historical data, and can typically facilitate solving the resultant optimization problems. Hence, they are naturally applicable for the energy harvesting system as well. The polyhedral set (3) *can be utilized whenever the upper and lower limits of the RES generation are available for each individual slots and subhorizons. In contrast, the covariance of the forecasting error is required to form the ellipsoidal set* (4)*.*

Remark 2 (Offline Vis-à-Vis Online Optimization): In this paper, we leverage an offline optimization method to decide the optimal transmitting power allocated in each time slot based on the knowledge of the forested RES amounts. Yet, such a historical-data-based inference scheme could possibly result in undesirable errors when compared to approaches using real-time data. An efficient way to improve system's operation is to adjust the predicted RES amounts according to real-time values and make the resource allocation decisions via an online optimization method, which leads to a more complicated problem. This will be an interesting direction to pursue in our future works.

C. Energy Storage Model

On-site storage units (e.g., battery banks) are available at the BS as a standby energy source. Let $0 \le C_t \le C^{\max}$ represent the state of charge (SoC) of the battery at the beginning of slot t, where $C^{\max}$ is the storage capacity. Further denote the power delivered to or drawn from the storage at slot t as $P_{b,t}$, which amounts to either charging ($P_{b,t} > 0$) or discharging ($P_{b,t} < 0$). The SoC dynamics can be captured by the following difference equation

$$C_t = C_{t-1} + P_{b,t}, \quad t \in \mathcal{T}. \tag{5}$$

Per slot t at most a fraction ϖ of the stored energy C_{t-1} is available for discharging. Hence, the power (dis-)charging amount is bounded by

$$P_b^{\min} \le P_{b,t} \le P_b^{\max} \tag{6}$$

$$-\varpi C_{t-1} \le P_{b,t} \tag{7}$$

where $P_b^{\min} < 0$ and $P_b^{\max} > 0$, while $\varpi \in (0, 1]$ denotes the battery efficiency.

Remark 3 (Battery Discharging Upper Bound): The battery efficiency ϖ is imposed to ensure that the energy withdrawn from the battery does not exceed its energy level. For simplicity and without loss of generality, this discharging upper bound is modeled as a fraction of the stored energy, which was referred as "energy causality" in [23]. Our proposed algorithm can be utilized to obtain the optimal solution for more general cases of the upper bound. Interested readers are referred to a thorough study of batteries in [24].

D. Energy Cost Model

For each slot t, the total energy consumption $P_{g,t} = P_c + P_{x,t}/\xi$ includes the transmitting power $P_{x,t}$, and a constant part $P_c > 0$, that is consumed by other components including air conditioning, data processor, and circuits [15]. The power amplifier efficiency $\xi > 0$ can be set to be one without loss of generality. We further assume that $P_{g,t}$ is bounded by $P_g^{\max}$.

In addition to the harvested RES, the main grid can also support the BS energy demand. Given the required energy $P_{g,t}$, the harvested energy E_t, and the battery charging energy $P_{b,t}$, the shortage energy that can be purchased from the grid is $[P_{g,t} - E_t + P_{b,t}]^+$; or, the surplus energy (when the harvested energy is abundant) that can be sold back to the grid is $[E_t - P_{g,t} - P_{b,t}]^+$, where $[a]^+ := \max\{a, 0\}$. Note that both the shortage and surplus energy are non-negative, and we can have at most one of them to be positive at any time t.

Let α_t and β_t denote the buying and selling prices, respectively. To avoid meaningless buy-and-sell activities of the BSs for profit, we shall have $\alpha_t > \beta_t$ for all t. Assuming that the prices α_t and β_t are perfectly known *a priori*, the *worst-case transaction cost* across all scheduling horizons is given by

$$G(\{P_{g,t}\}, \{P_{b,t}\}) := \max_{\mathbf{e}\in\mathcal{E}} \sum_{t=1}^{T} \Big(\alpha_t [P_{g,t} - E_t + P_{b,t}]^+ - \beta_t [E_t - P_{g,t} - P_{b,t}]^+ \Big). \tag{8}$$

If G_c denotes the budget of the transaction cost, it then holds that $G(\{P_{g,t}\}, \{P_{b,t}\}) \le G_c$.

III. Optimal Resource Allocation

Based on the models presented in Section II, we will optimize here the allocation of resources for the smart-grid powered MIMO BCs. Specifically, through finding the

optimal transmit covariance matrices $\{\Gamma_{k,t}, \forall k, t\}$, transmit-power $\{P_{x,t}, \forall t\}$, and battery charging energy $\{P_{b,t}, \forall t\}$, the BS wishes to maximize the (weighted) total throughput of the downlink transmission, subject to a given budget of the worst-case transaction cost. Define $\Gamma_t := \{\Gamma_{k,t} \ \forall k\}$, and let $\mathbf{r}^B(\Gamma_t) := [r_1^B(\Gamma_t), \ldots, r_K^B(\Gamma_t)]'$ collect the achieved transmission rates for all the users. By introducing auxiliary variables $P_t := P_{g,t} + P_{b,t}$, the resource allocation task of interest can be formulated as the following optimization problem:

$$\max_{\{\Gamma_t, C_t, P_t, P_{x,t}, P_{b,t}\}} \sum_{k=1}^{K} [w_k \sum_{t=1}^{T} (r_k^B(\Gamma_t))] \tag{9a}$$

$$\text{s. t. } G(\{P_t\}) \leq G_c, \quad t \in \mathcal{T} \tag{9b}$$

$$P_t = P_{x,t} + P_{b,t} + P_c, \quad t \in \mathcal{T} \tag{9c}$$

$$P_c \leq P_c + P_{x,t} \leq P_g^{\max}, \quad t \in \mathcal{T} \tag{9d}$$

$$P_b^{\min} \leq P_{b,t} \leq P_b^{\max}, \quad t \in \mathcal{T} \tag{9e}$$

$$C_t = C_{t-1} + P_{b,t}, \quad t \in \mathcal{T} \tag{9f}$$

$$0 \leq C_t \leq C^{\max}, \quad t \in \mathcal{T} \tag{9g}$$

$$-\varpi C_{t-1} \leq P_{b,t}, \quad t \in \mathcal{T} \tag{9h}$$

$$\mathbf{r}^B(\Gamma_t) \in \mathcal{C}_{\text{BC}}(P_{x,t}; \mathcal{H}), \quad t \in \mathcal{T} \tag{9i}$$

where $\boldsymbol{w} := [w_1, \ldots, w_K]'$ collects the priority weights of all users. Solving (9) for all $\boldsymbol{w} \geq \mathbf{0}$ can yield all the boundary points of the achievable rate region.

Since the achievable rate $r_k^B(\Gamma_t)$ is generally non-concave, the problem (9) is non-convex. We next resort to the uplink-downlink duality and a "nested optimization" approach to reformulate (9) into a convex problem.

A. Convex Reformulation

We will first argue that $G(\{P_t\})$ in (9b) is convex. With $\delta_t := (\alpha_t - \beta_t)/2$ and $\phi_t := (\alpha_t + \beta_t)/2$, we can rewrite $G(\{P_t\})$ as

$$G(\{P_t\}) = \max_{\mathbf{e} \in \mathcal{E}} \sum_{t=1}^{T} \left(\delta_t |P_t - E_t| + \phi_t (P_t - E_t)\right).$$

Since $\alpha_t > \beta_t \geq 0$, we have $\phi_t > \delta_t > 0$. It is then clear that function $\delta_t |P_t - E_t| + \phi_t (P_t - E_t)$ is convex in P_t, whenever E_t is fixed. As a pointwise maximization of these convex functions, $G(\{P_t\})$ is also convex, even when the set $\mathcal{E}$ is non-convex [4], [25].

Remark 4 (Properties of the Cost Function): The condition $\alpha_t > \beta_t$ is sufficient but not necessary to guarantee that the function $G(\{P_t\})$ is convex. The cost function can take other forms as well. Our proposed method is still applicable as long as the cost function is convex with respect to its effective domain. This includes the case when the selling prices exceed the purchase prices. If the cost function is not convex, a new solver is needed for the resulting nonconvex problem.

Relying on uplink-downlink duality [26], the BC capacity region $\mathcal{C}_{\text{BC}}(P_{x,t}; \mathcal{H})$ can be alternatively characterized by the capacity regions of a set of "dual" multi-access channels (MACs). In the dual MAC, the received signal is

$$\boldsymbol{y}(t) = \sum_{k=1}^{K} \boldsymbol{H}_k^{\dagger} \boldsymbol{x}_k(t) + \boldsymbol{z}(t)$$

where $\boldsymbol{x}_k(t)$ is the transmitted signal by user k, and $\boldsymbol{z}(t)$ is additive complex-Gaussian with zero mean and identity covariance matrix $\mathbf{I}$. Let $\mathbf{Q}_k := \mathbb{E}[\boldsymbol{x}_k \boldsymbol{x}_k^{\dagger}] \succeq \mathbf{0}$ denote the transmit covariance matrix for user k, and $\mathbf{P} := [P_1, \ldots, P_K]'$ collect the transmit-power budgets for users. For a given $\mathbf{P}$, the MAC capacity region is given by

$$\mathcal{C}_{\text{MAC}}(\mathbf{P}; \mathcal{H}^{\dagger}) = \bigcup_{\{\mathbf{Q}_k: \, \text{tr}(\mathbf{Q}_k) \leq P_k, \, \forall k\}} \Big\{(r_1, \ldots, r_K) : \sum_{k \in \mathcal{S}} r_k \leq \log \left| \mathbf{I} + \sum_{k \in \mathcal{S}} \mathbf{H}_k^{\dagger} \mathbf{Q}_k \mathbf{H}_k \right|, \ \forall \mathcal{S} \subseteq \{1, \ldots, K\} \Big\}.$$

The BC capacity region (2) equals the union of the above MAC capacity regions corresponding to all power vectors $\mathbf{P}$ satisfying $\sum_{k=1}^{K} P_k \leq P_{x,t}$ [11]; that is

$$\mathcal{C}_{\text{BC}}(P; \mathcal{H}) = \bigcup_{\{\mathbf{P}: \sum_{k=1}^{K} P_k \leq P_{x,t}\}} \mathcal{C}_{\text{MAC}}(\mathbf{P}; \mathcal{H}^{\dagger}) := \mathcal{C}_{\text{MAC}}(P; \mathcal{H}^{\dagger}). \tag{10}$$

With $R(P_{x,t}) := \max_{\mathbf{r}^B(\Gamma_t) \in \mathcal{C}_{\text{BC}}(P_{x,t}; \mathcal{H})} \sum_{k=1}^{K} w_k r_k^B(\Gamma_t)$, we then have the following lemma [11]

Lemma 1: The function $R(P_{x,t})$ can be alternatively obtained as the optimal value of the following problem:

$$\max_{\mathbf{Q}_k \succeq 0} \sum_{k=1}^{K} (w_{\pi(k)} - w_{\pi(k+1)}) \log \left| \mathbf{I} + \sum_{u=1}^{k} \mathbf{H}_{\pi(u)}^{\dagger} \mathbf{Q}_{\pi(u)} \mathbf{H}_{\pi(u)} \right| \tag{11a}$$

$$\text{s. t. } \sum_{k=1}^{K} \text{tr}(\mathbf{Q}_k) = P_{x,t} \tag{11b}$$

where π is the permutation of user indices $\{1, \ldots, K\}$ such that $w_{\pi(1)} \geq \cdots \geq w_{\pi(K)}$, and $w_{\pi(K+1)} = 0$.

Remark 5 (Validity of the Uplink-Downlink Duality With RES): The information-theoretic uplink-downlink duality was established under a sum-power constraint; i.e., it holds when the multi-access channel (uplink) and broadcast channel (downlink) have the same sum-power budget. Such a duality holds regardless of the types of power supply. Integration of the RES with persistent power supply would only change the optimal allocation of the sum-power per slot.

Using $R(P_{x,t})$, problem (9) can be converted into the following optimal sum-power allocation problem for an equivalent "point-to-point" link:

$$\max_{\{C_t, P_t, P_{x,t}, P_{b,t}\}} \sum_{t=1}^{T} R(P_{x,t}) \quad \text{s. t. (9b)} - \text{(9h)}. \tag{12}$$

The objective in (12) is concave per Lemma 1 while all constraints are convex; hence, (12) is a convex program.

In the ensuing sections, a nested optimization procedure will be developed for obtaining the optimal strategy.

Specifically, we will first solve (12) to obtain the optimal $\{C_t^*, P_t^*, P_{x,t}^*, P_{b,t}^*\}$. Then given $\{P_{x,t}^*\}_t$, we will solve the convex problem (11) to obtain the optimal "virtual" uplink covariance matrices $\mathbf{Q}_k(P_{x,t}^*)$, $\forall k$. Finally, the desired downlink covariance matrices $\Gamma_{t,k}^*$ will be recovered from $\mathbf{Q}_k(P_{x,t}^*)$ using the uplink-downlink duality.

B. Lagrange Dual Approach

We next develop a Lagrange dual approach to solve (12). Let $\{\lambda_t\}_{t\in\mathcal{T}}$ denote the Lagrange multipliers associated with constraints (9c), and μ the multiplier with (9b). Letting $\boldsymbol{Z} := \{C_t, P_t, P_{x,t}, P_{b,t}, \forall t\}$ and $\boldsymbol{\Lambda} := \{\mu, \lambda_t, \forall t\}$, the partial Lagrangian function of (12) is

$$L(\boldsymbol{Z}, \boldsymbol{\Lambda}) := \sum_{t\in\mathcal{T}}\Big[R(P_{x,t}) + \lambda_t\big(P_t - P_{x,t} - P_{b,t} - P_c\big)\Big] - \mu\big(G(\{P_t\}) - G_c\big). \tag{13}$$

The Lagrangian dual function is then obtained as

$$D(\boldsymbol{\Lambda}) := \max_{\boldsymbol{Z}} \; L(\boldsymbol{Z}, \boldsymbol{\Lambda}), \quad \text{s. t. (9d)} - \text{(9h)} \tag{14}$$

and the dual problem of (12) is:

$$\min_{\boldsymbol{\Lambda}} \; D(\boldsymbol{\Lambda}). \tag{15}$$

Subgradient Iterations: For the dual problem (15), a subgradient descent method can be employed to obtain the optimal $\boldsymbol{\Lambda}^*$. This amounts to running the iterations

$$\lambda_t(j+1) = \lambda_t(j) - a(j)g_{\lambda_t}(j), \quad \forall t \tag{16a}$$

$$\mu(j+1) = [\mu(j) - a(j)g_\mu(j)]^+ \tag{16b}$$

where j is the iteration index, and $a(j) > 0$ is an appropriate stepsize. The subgradient $\boldsymbol{g}(j) := [g_{\lambda_t}(j), g_\mu(j)]'$ can then be expressed as

$$g_{\lambda_t}(j) = P_t(j) - P_{b,t}(j) - P_{x,t}(j) - P_c \tag{17a}$$

$$g_\mu(j) = G_c - G(\{P_t(j)\}) \tag{17b}$$

where $P_t(j)$, $P_{b,t}(j)$, and $P_{x,t}(j)$ are given by

$$\{P_t(j)\}_{t=1}^T \in \arg\max_{\{P_t\}} \Big[\sum_{t=1}^T \lambda_t(j)P_t - \mu(j)G(\{P_t\})\Big] \tag{18a}$$

$$\{P_{b,t}(j)\}_{t=1}^T \in \arg\max_{\{P_{b,t}, C_t\}} \sum_{t=1}^T [-\lambda_t(j)P_{b,t}] \quad \text{s. t. (9e)} - \text{(9h)} \tag{18b}$$

$$\{P_{x,t}(j)\}_{t=1}^T \in \arg\max_{\{P_{x,t}\}} \sum_{t=1}^T [R(P_{x,t}) - \lambda_t(j)P_{x,t}] \quad \text{s. t. (9d)}. \tag{18c}$$

Solving the Subproblems: Subproblems (18b) are simple linear programs (LPs) over the variables $\{P_{b,t}, C_t\}_{t=1}^T$, which can be obtained by off-the-shelf LP solvers.

To solve the subproblems (18c), first define $f(\lambda_t(j)) := \max_{P_{x,t}\geq 0} \; R(P_{x,t}) - \lambda_t(j)P_{x,t}$, and

$$F(\mathbf{Q}) = \sum_{k=1}^K (w_{\pi(k)} - w_{\pi(k+1)}) \log\left|\mathbf{I} + \sum_{u=1}^k \mathbf{H}_{\pi(u)}^\dagger \mathbf{Q}_{\pi(u)}\mathbf{H}_{\pi(u)}\right|.$$

Then by Lemma 1, we have

$$\begin{aligned} f(\lambda_t(j)) &= \max_{P_{x,t}\geq 0} \Big[\max_{\sum_{k=1}^K \mathrm{tr}(\mathbf{Q}_k) = P_{x,t}} F(\mathbf{Q}) - \lambda_t(j)P_{x,t}\Big] \\ &= \max_{\mathbf{Q}\geq 0} \Big[F(\mathbf{Q}) - \lambda_t(j)\sum_{k=1}^K \mathrm{tr}(\mathbf{Q}_k)\Big]. \end{aligned} \tag{19}$$

Problem (19) is a convex program which can be solved using interior-point algorithms in polynomial time. We can subsequently determine $P_{x,t}^* = \min\{P_g^{\max} - P_c, \sum_{k=1}^K \mathrm{tr}(\mathbf{Q}_k^*(\lambda_t(j)))\}$ with the optimal solution $\mathbf{Q}^*(\lambda_t(j))$.

The non-differentiability of $G(\{P_t\})$ due to the absolute value operator and pointwise maximization renders the subproblem (18a) challenging in spite of its convexity. To cope with this issue, we resort to the proximal bundle method to efficiently obtain $\{P_t(j)\}_{t=1}^T$; see details in [20].

C. Optimal Broadcasting Solution

With the optimal sum transmit power $P_{x,t}^*$ per time slot t, the optimal transmit-covariance matrices $\{\Gamma_{t,k}^*, \forall k\}$ can be alternatively obtained by solving (11). The optimal solutions $\{\mathbf{Q}_k(P_{x,t}^*)\}_{k\in\mathcal{K}}$ to problem (11) can be obtained in polynomial time, from which we can find $\Gamma_{t,k}^*$ using the uplink-downlink duality as follows. First, let us define two matrices for $k = 1, \ldots, K$

$$\mathbf{A}_k = \mathbf{I} + \mathbf{H}_{\pi(k)}\left(\sum_{u=1}^{k-1}\Gamma_{i,\pi(u)}^*\right)\mathbf{H}_{\pi(k)}^\dagger \tag{20}$$

$$\mathbf{B}_k = \mathbf{I} + \sum_{u=k+1}^K \Big(\mathbf{H}_{\pi(u)}^\dagger \mathbf{Q}_{\pi(u)}^*(P_i^*)\mathbf{H}_{\pi(u)}\Big). \tag{21}$$

Then, we can find the optimal $\{\Gamma_{t,\pi(k)}^*\}_{k\in\mathcal{K}}$ as

$$\Gamma_{t,\pi(k)}^* = \mathbf{B}_k^{-\frac{1}{2}}\mathbf{F}_k\mathbf{G}_k^\dagger\mathbf{A}_k^{\frac{1}{2}}\mathbf{Q}_{\pi(k)}^*(P_{x,t}^*)\mathbf{A}_k^{\frac{1}{2}}\mathbf{G}_k\mathbf{F}_k^\dagger\mathbf{B}_k^{-\frac{1}{2}} \tag{22}$$

where $\mathbf{F}_k$ and $\mathbf{G}_k$ are obtained by decomposing the effective channel using singular value decomposition: $\mathbf{B}_k^{-\frac{1}{2}}\mathbf{H}_{\pi(k)}^\dagger\mathbf{A}_k^{-\frac{1}{2}} = \mathbf{F}_k\mathbf{S}\mathbf{G}_k^\dagger$ with a square and diagonal $\mathbf{S}$ [11].

It is worth stressing that

$$\Gamma_{t,\pi(1)}^* = \mathbf{B}_1^{-\frac{1}{2}}\mathbf{F}_1\mathbf{G}_1^\dagger\mathbf{Q}_{\pi(1)}^*(P_{x,t}^*)\mathbf{G}_1\mathbf{F}_1^\dagger\mathbf{B}_1^{-\frac{1}{2}}$$

which only requires knowledge of $\mathbf{Q}_{\pi(1)}^*(P_{x,t}^*)$. To obtain $\{\Gamma_{t,\pi(k)}^*\}_{k=2}^K$, the quantities $\mathbf{A}_k$ and $\Gamma_{t,\pi(u)}$ for $u = 1, \ldots, k-1$ are needed. Clearly, all $\Gamma_{t,k}^*$ can be found in such a sequential way. It then readily follows that the optimal broadcasting schedule $\{\Gamma^*\}$ for problem (9) can be obtained with a low complexity.

Remark 6 (Structural Properties of the Optimal Solution): Rather than restraining the transaction cost for each time slot, the cost function $G(\{P_t\})$ is upper bounded by a given budget for the entire scheduling horizon when maximizing the sum-rate of the MIMO BC. Hence, the BS tends to buy more energy from the grid when the electricity price is relatively low to supply data transmission and to charge the batteries. While the electricity price is high, the BS is inclined to employ its stored energy to power itself and even sell surplus energy to the grid to reduce the cost. As corroborated by the numerical results

Algorithm 1 Optimal Resource Allocation for Smart-Grid Powered MIMO BCs

1: **Initialize** $\mathbf{\Lambda}(0) \geq \mathbf{0}$.
2: Given $\mathbf{\Lambda}(j)$, solve subproblems (18a), (18b), and (19) yielding $\{P_t(j), P_{b,t}(j), P_{x,t}(j)\}_{t=1}^T$.
3: Update $\mathbf{\Lambda}(j+1)$ via (16).
4: Let $j = j+1$, and repeat steps 2 and 3 until convergence.
5: Obtain the optimal solutions $\mathbf{\Lambda}^*$ and $\{P_t^*, P_{x,t}^*, P_{b,t}^*, C_t^*\}$.
6: Given $\{P_{x,t}^*\}$, solve (11) and obtain $\Gamma_{t,k}^*$ using (22).

in Fig. 10, the optimal $\{P_{b,t}^*, C_t^*\}$ yielded by the proposed algorithm follow such a structure.

D. Convergence of the Subgradient Solver

The procedures of our proposed approach are summarized in Algorithm 1. This algorithm is guaranteed to converge to the optimal solution of (9). Specifically, for a constant stepsize $a(j) = a$, the subgradient iterations (16) are guaranteed to converge to a neighborhood of the optimal $\mathbf{\Lambda}^*$ starting from any initial point $\mathbf{\Lambda}(0)$. The size of the neighborhood is proportional to the stepsize a. If a sequence of non-summable diminishing stepsizes $\lim_{j\to\infty} a(j) = 0$ and $\sum_{j=0}^{\infty} a(j) = \infty$ is adopted, the iterations (16) will converge to the exact $\mathbf{\Lambda}^*$ as $j \to \infty$ [27].

Since there is no duality gap between the convex primal problem (12) and its dual (15), the optimal solution to the original problem (9) is subsequently obtained upon convergence of $\mathbf{\Lambda}^*$.

IV. Generalizations

The proposed approach can be generalized to account for time-varying MIMO BC, and on-off transmissions.

A. Time-Varying Channel

Suppose the channel states are time varing in general. Let $\mathcal{H}_t := \{\mathbf{H}_{t,1}, \ldots, \mathbf{H}_{t,K}\}$ collect the channel per epoch t. As with (9), we can formulate the weighted-sum throughput maximization problem as

$$\max_{\Gamma} \quad \sum_{k=1}^{K}[w_k \sum_{t=1}^{T}(r_k^B(\Gamma_t))] \tag{23a}$$

$$\text{s. t.} \quad (9b) - (9h)$$

$$\mathbf{r}^B(\Gamma_t) \in \mathcal{C}_{\text{BC}}(P_{x,t}; \mathcal{H}_t), \quad t = 1, \ldots, T. \tag{23b}$$

where the BC capacity region $\mathcal{C}_{\text{BC}}(P_{x,t}; \mathcal{H}_t)$ varies with the channel state $\mathcal{H}_t$ for $t = 1, \ldots, T$.

Define $R(P_{x,t}) := \max_{\mathbf{r}^B(\Gamma_t)\in\mathcal{C}_{\text{BC}}(P_{x,t};\mathcal{H}_t)} \sum_{k=1}^{K} w_k r_k^B(\Gamma_t)$. By Lemma 1, $R(P_{x,t}; \mathcal{H}_t)$ is a strictly concave function of $P_{x,t}$. Using $R(P_t; \mathcal{H}_t)$, we can convert (23) into

$$\max_{\{C_t, P_t, P_{x,t}, P_{b,t}\}} \sum_{t=1}^{T} R(P_{x,t}) \tag{24}$$

$$\text{s. t.} \quad (9b) - (9h).$$

Since problem (24) is still convex, the proposed dual-subgradient approach readily carries over to yield the optimal $\{C_t^*, P_t^*, P_{x,t}^*, P_{b,t}^*\}$. Note that for time-varying channels, the optimal transmit-power allocation exhibits a "water-filling" structure; that is, higher power are allocated to channels with better quality [1], [11]. Given $P_{x,t}^*$ per slot, the optimal transmit covariance matrices $\Gamma_{t,k}^*$ can be subsequently determined, as specified in Section III-D.

B. On-Off Transmissions

When circuit-power P_c is positive, it was shown that a bursty (i.e., on-off) transmission can be adopted to achieve a higher transmission rate under the same power budget [11], [28], [29]. For the MIMO BC case here, this implies that the BS may be turned on for only a portion of a slot. Consider the time-invariant channel case for simplicity. Let $l_t \in [0, 1]$ denote the duration of the on-period of the BS per slot t, and note that the notations of "energy" and "power" become different after introducing l_t.

Assume $P_c = 0$ when the BS is turned off, and the battery can always be (dis)charged during the entire time slot. Per slot t, let $P_{b,t}$ denote the energy delivered to or drawn from the batteries. With the duration of "on" period l_t, the total energy consumption at the BS becomes $P_{g,t}l_t = (P_{x,t} + P_c)l_t$. Upon redefining the *worst-case transaction cost*

$$G_l(\{P_{g,t}\}, \{P_{b,t}\}, \{l_t\}) := \max_{\mathbf{e}\in\mathcal{E}} \sum_{t=1}^{T} \Big(\alpha_t[P_{g,t}l_t - E_t + P_{b,t}]^+ - \beta_t[E_t - P_{g,t}l_t - P_{b,t}]^+\Big), \tag{25}$$

problem (12) can be rewritten as

$$\max_{\{C_t, P_{g,t}, P_{x,t}, P_{b,t}, l_t\}} \quad \sum_{t=1}^{T}[R(P_{x,t})l_t] \tag{26a}$$

$$\text{s. t.} \quad (9e) - (9h)$$

$$G_l(\{P_{g,t}\}, \{P_{b,t}\}, \{l_t\}) \leq G_c \tag{26b}$$

$$P_c l_t \leq P_{g,t} l_t \leq P_g^{\max} \tag{26c}$$

$$0 \leq l_t \leq 1. \tag{26d}$$

Problem (26) is clearly non-convex. However, it can be reformulated into a convex program through a change of variables [11]. Upon redefining $\Psi_t := P_{g,t}l_t$ and $P_t := \Psi_t + P_{b,t}$, we can rewrite (25) as

$$G_l(\{P_t\}) := \max_{\mathbf{e}\in\mathcal{E}} \sum_{t=1}^{T} \Big(\alpha_t[P_t - E_t]^+ - \beta_t[E_t - P_t]^+\Big). \tag{27}$$

Then (26) can be reformulated as:

$$\max_{\{C_t, P_{b,t}, P_t, l_t, \Psi_t\}} \quad \sum_{t=1}^{T}[l_t R(\frac{\Psi_t}{l_t} - P_c)] \tag{28a}$$

$$\text{s. t.} \quad (9e) - (9h)$$

$$P_t = \Psi_t + P_{b,t} \tag{28b}$$

$$G_l(\{P_t\}) \leq G_c \tag{28c}$$

$$0 \leq l_t \leq 1 \tag{28d}$$

$$P_c l_t \leq \Psi_t \leq P_g^{\max}. \tag{28e}$$

Algorithm 2 Optimal Solution for On-Off Transmission (29)

1: **Initialize** $0 \leq l_t \leq 1$.
2: Given $l_t(i)$, solve the problem (19) yielding $\Psi_t(i)$.
3: Obtain P_{ee}^*.
4: Compare $\Psi_t(i)$ with P_{ee}^* and update $l_t(i+1)$ accordingly.
5: Let $i = i+1$, and repeat steps 2 and 4 until convergence.
6: Obtain the optimal solutions $\{l_t^*, \Psi_t^*\}$ for subproblems (29).

Because $R(P_{x,t})$ is concave in $P_{x,t}$, its "perspective" $l_t R(\frac{\Psi_t}{l_t} - P_c)$ is a jointly concave function of (Ψ_t, l_t) [25]. As all constraints become convex too, it follows that (28) is a convex problem. Hence, it can be readily solved by modifying the proposed Lagrange dual based subgradient approach. The procedures and formulas are similar to those in Section III-B except for subproblems (18c), which become

$$\{\Psi_t(j)\}_{t=1}^T \in \arg \max_{\{\Psi_t, l_t\}} \sum_{t=1}^T [l_t R(\frac{\Psi_t}{l_t} - P_c) - \lambda_t(j)\Psi_t] \quad \text{s. t. (28d) and (28e)} \tag{29}$$

where $\{\lambda_t, \mu, \forall t\}$ collect the Lagrange multipliers associated with constraints (28b) and (28c).

Since subproblems (29) are jointly convex in $\{l_t, \Psi_t\}$, the optimal solution can be achieved through the alternating optimization method, which amounts to running the iterations according to the following two steps: s1) set a value for l_t to obtain Ψ_t; and s2) find l_t with the obtained Ψ_t. Step s1), it is just the same we used to solve subproblems (18c), by transforming the problem into a convex program (19), which can be readily and efficiently solved. Thus, we arrive at $\Psi_t = \min\{P_g^{\max}, l_t(\sum_{k=1}^K \text{tr}(\boldsymbol{Q}_k^*) + P_c)\}$.

In order to find the optimal l_t given Ψ_t, we rely on the so-termed bits-per-Joule maximizing power P_{ee}^* [11]. Specifically, l_t can be obtained by comparing Ψ_t with P_{ee}^* as: $l_t = \frac{\Psi_t}{P_{ee}^* + P_c}$ if $\Psi_t < P_{ee}^* + P_c$; otherwise, $l_t = 1$. After convergence, we can obtain the globally optimal solution $\{l_t^*, \Psi_t^*\}$ for subproblems (29).

The described procedures are summarized in Algorithm 2, where i is the iteration number for the subproblems. With the optimal $\{C_t^*, P_{b,t}^*, P_t^*, l_t^*, \Psi_t^*\}$ for (28), the resulting on-off transmission strategy can further improve the total throughput, at the cost of more sophisticated coordination and signaling between the BS and users.

V. Numerical Tests

In this section, simulated tests are presented to verify the performance of the proposed approach. The Matlab-based modeling package `CVX 2.1` [30] with the solvers `MOSEK 7.0` [31] and `Sedumi 1.02` [32] are used to specify and solve the resulting optimization problems. All numerical tests are implemented on a computer workstation with Intel cores 2.0 GHz and 32 GB RAM.

We first consider a MIMO downlink system where the BS has $N_t = 2$ antennas, and $K = 2$ mobile users each equipped with $N_r = 2$ antennas. All wireless channels are generalized according to the models in [33, Ch. 2], where $H_k = \sqrt{\gamma_k}\tilde{H}_k$, with γ_k the large-scale fading coefficient, and $\tilde{H}_k$ the estimated flat Rayleigh fading channel coefficient matrix for user k. We set $\gamma_1 = 2$ and $\gamma_2 = 1$. The noises are modeled as circularly-symmetric Gaussian random vectors. The system bandwidth is 10 MHz. The total scheduling horizon is $T = 8$ hours. Parameters including the limits of $P_{g,t}$, C_t, $P_{b,t}$, the discharging efficiency ϖ, and the transaction cost budget G_c are listed in Table I. A polyhedral uncertainty set (3) with a single sub-horizon is considered for the RES. Bounds of the forecasted energy are set as $\overline{E}_t = 10\underline{E}_t$, where the lower bounds $\{\underline{E}_t\}_{t\in\mathcal{T}}$ are listed in Table II. The transaction prices are set equal to $\beta_t = r\alpha_t$ with $r = 0.7$, and $\{\alpha_t\}_{t\in\mathcal{T}}$ are also given in Table II.

TABLE I

Generating Capacity, Battery Initial Energy and Capacity, Charging Limits and Efficiency, Maximum Power Cost

Parameter (Unit)	$P_g^{\max}$ (KW)	C_0 (KW)	$C^{\max}$ (KW)	$P_b^{\min}$ (KW)	$P_b^{\max}$ (KW)	ϖ (N/A)	G_c ($)
Value	40	5	30	-10	10	0.95	20

TABLE II

Lower Bounds of the Forecasted Energy (KW) and Energy Purchase Prices ($/KWh)

Slot	1	2	3	4	5	6	7	8
$\underline{E}_t$	2.47	2.27	2.18	1.97	2.28	2.66	3.1	3.38
α_t	0.402	0.44	0.724	1.32	1.166	0.798	0.506	0.468

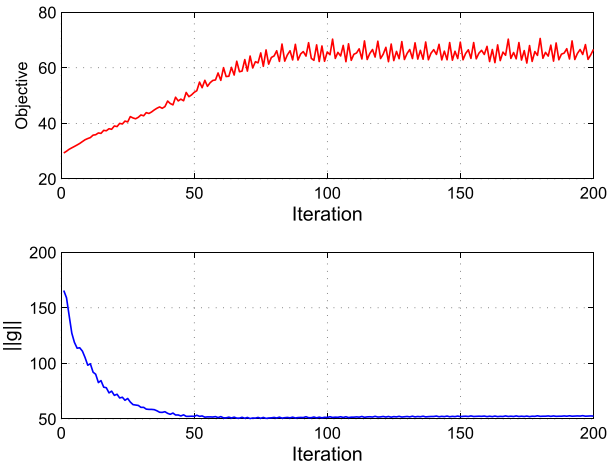

Fig. 2. Convergence of the objective value and the norm of Lagrange multipliers.

Convergence of the objective value (12), and the ℓ_2-norm of the subgradient of the Lagrange multipliers (17) are shown in Fig. 2. Clearly, both metrics converge very fast within about a hundred iterations, which justifies the validity of the dual decomposition. Since we adopt a constant stepsize $a = 0.001$ for the subgradient iterations, the objective value converges to a neighborhood of the optimal solution with some oscillations. A diminishing stepsize can be used to guarantee the convergence to the optimal solution.

By changing the weight $\boldsymbol{w} := [w_1, w_2]'$ such that $w_1 + w_2 = 1$, and $w_1, w_2 \in [0, 1]$, Algorithm 1 is implemented

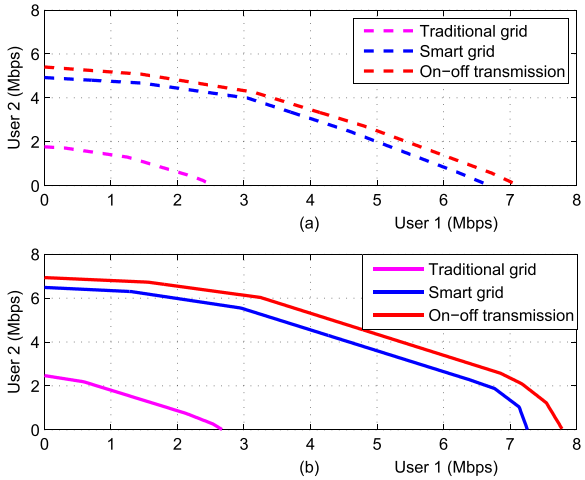

Fig. 3. Capacity regions for time-invariant MIMO BCs. (a) $N_t = 2$. (b) $N_t = 4$.

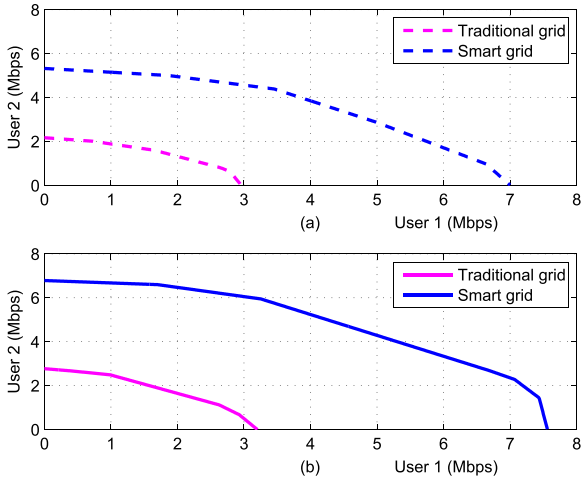

Fig. 4. Capacity regions for time-varying MIMO BCs. (a) $N_t = 2$. (b) $N_t = 4$.

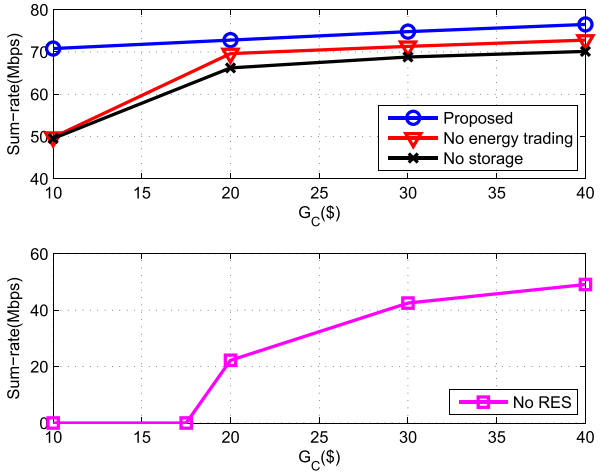

Fig. 5. Sum-rates for MIMO BCs subject to G_c ($K = 10$, $N_t = 2$).

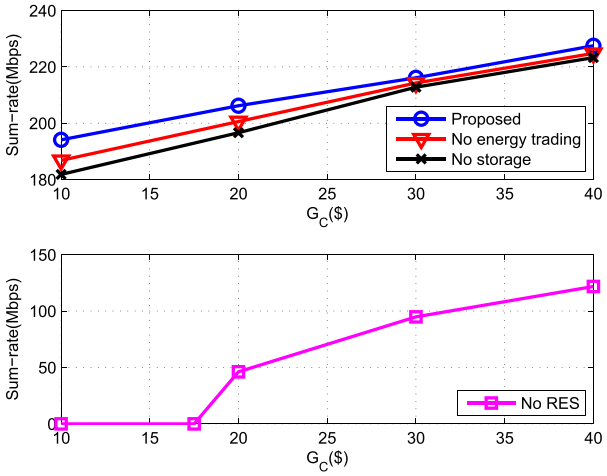

Fig. 6. Sum-rates for MIMO BCs subject to G_c ($K = 10$, $N_t = 10$).

to find the boundary of a time-invariant MIMO BC capacity region as shown in Fig. 3. The counterpart of the system without RES and two-way energy trading is included as a benchmark. The on-off transmission scheme is also considered for the time-invariant channel. We test two scenarios: $N_t = 2$ and $N_t = 4$, for all three cases, which are depicted in Fig. 3(a) and Fig. 3(b), respectively. It can be clearly seen that the achievable rate limits are more than doubled when the system is powered by RES and scheduled by the local controller. This is because the BS can utilize its harvested energy to provide extra power for data transmission. As for the on-off transmission strategy, the achievable rate limits for both users are about 0.5 Mbps larger than those of the proposed system as shown in Fig. 3. Energy usage efficiency is improved because the BS can adopt bursty transmissions to deliver more bits per Joule [28]. It can be seen that when the number of transmitting antennas N_t doubles, the capacity region for the MIMO BC becomes much larger because the spatial multiplexing gain increases per user.

Fig. 4 depicts the capacity regions of a time-varying MIMO BC, where each entry of the channel matrix $\{\mathbf{H}_k\}_{k=1,2}$ is a zero-mean complex Gaussian random variable with unit variance per slot t. Large-scale fading coefficients are selected as before. Note that the sample average sum-rate is based on 100 different channel realizations. Due to the dynamic management of energy and time-varying channels, the corresponding capacity regions are larger than those of a time-invariant channel.

Next, we consider a total of $K = 10$ users, each equipped with $N_r = 2$ antennas, served by a small system ($N_t = 2$) or a large system ($N_t = 10$). All users's priority weights are set as $w_k = 1, \forall k$, for convenience. The broadcast channels of both systems are time-invariant. Users are split into 3 groups (each group has 3 or 4 users) according to their distances from the BS, where the large-scale fading coefficients are 2, 1, and 0.5, respectively. In Figs. 5 and 6, we depict MIMO BC sum-rates with different budgets of the worst-case transaction cost to further demonstrate the merits of the proposed framework. The considered power-grid configurations include (C1) a system with RES and storage has no two-way energy trading; (C2) the BS has only RES; and (C3) no RES, battery and energy trading. It is clearly seen that the sum-rate of the proposed system is the largest, while that

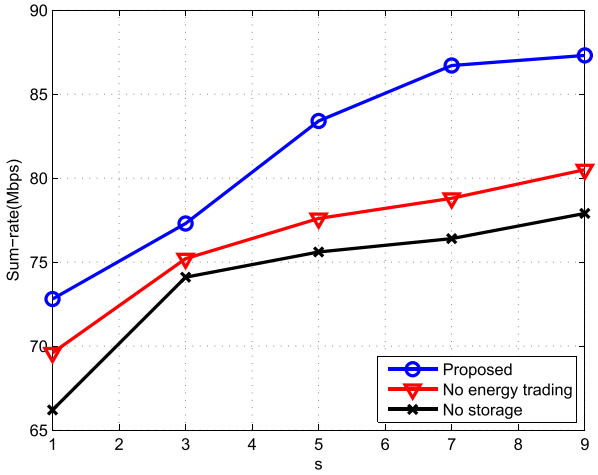

Fig. 7. Sum-rates for MIMO BCs subject to $\underline{E}_t$ ($K = 10$, $N_t = 2$).

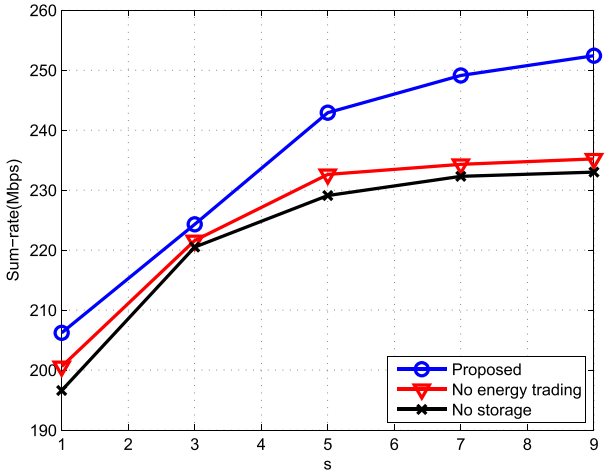

Fig. 8. Sum-rates for MIMO BCs subject to $\underline{E}_t$ ($K = 10$, $N_t = 10$).

of the conventional system is the smallest due to lack of RES facilities. As a matter of fact, sum-rate of the traditional-grid-powered BC depends totally on the transaction cost budget, and when the budget is less than \$17.5, the BS cannot even afford the circuit-power cost P_c. It will therefore be turned off, resulting in a null sum-rate.

It is also observed that when $G_c = \$40$, sum-rate of the proposed system is about 25 Mbps higher than that of the conventional system. It is 5 Mbps higher than those of the other two competing configurations, and the sum-rate difference reaches 20 Mbps when G_c is reduced to \$10, where sum-rate of the proposed system remains large, while those of the three competing systems drop dramatically due to the limited capabilities of RES and energy trading. Merits of the proposed system are evident, especially when the cost budget is very small, because the BS can consume more of its harvested or stored energy, and buy less electricity from the main grid under such circumstances. Sum-rates of all four systems increase with the increasing cost budget since the BS can buy more energy from the grid. But when the budget is large enough to afford any amount of energy, the sum-rate increases slowly with the increasing of G_c, for the sum-rate is then bounded by the transmit power budget $P_g^{\max}$.

For further illustration, we depict the influence of the amount of harvested energy on the sum-rates in Figs. 7 and 8. Since the traditional grid (C3) does not have RES devices, it will not be included for comparison. The lower bound of the RES uncertainty set is $s\underline{E}_t$, and the upper bound is $10s\underline{E}_t$, where values of $\{\underline{E}_t\}_{t\in\mathcal{T}}$ are listed in Table II. Values of other parameters are listed in Tables I and II. It is clearly seen that sum-rates of the three systems increase as s increases. Because the harvested energy can make up for the limited amount of energy the BS purchases from the grid with a small budget, say, \$20, the sum-rate is higher. Sum-rate of the proposed system is the largest and becomes much larger than those of the other two configurations because it can save superfluous energy for later use and even sell it to the main grid to reduce operational cost. The sum-rate difference can reach $15-20$ Mbps in the end. This demonstrates clearly that the proposed system is economical and ecological.

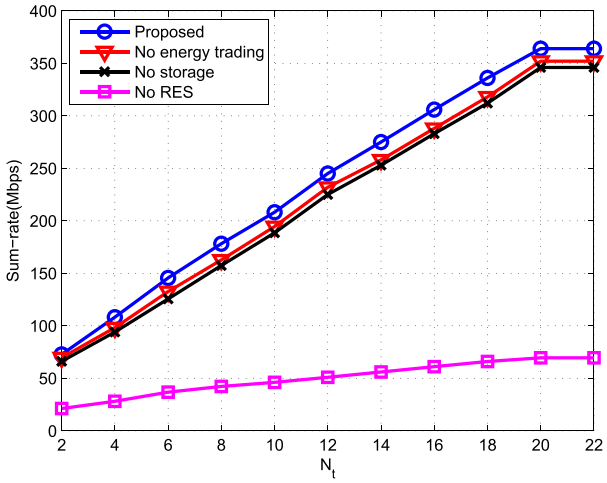

Fig. 9. Sum-rates for MIMO BCs subject to N_t ($K = 10$).

Fig. 9 illustrates the effect of the number of transmitting antennas N_t on sum-rates of the time-invariant MIMO BCs. Clearly, sum-rates of the MIMO BCs increase almost linearly with the number of transmit antennas. This is consistent with the theoretical result that the capacity of MIMO BC scales linearly with the minimum of total transmit- and receive-antennas. Note that since we have $K = 10$ users and each user is equipped with 2 antennas, there are a total of 20 receive antennas in the system. When we have $N_t > 20$ transmit antennas, the total degree of freedoms and the capacity of the MIMO BC are in fact bounded by the number of receive antennas. Hence, the system sum-rates do not increase for $N_t > 20$. It is also observed that sum-rate differences between the proposed scheme and the three baseline schemes are 10 Mbps, 20 Mbps and 90 Mbps, respectively. Merits of BS integrated with smart-grid capabilities are once again verified.

Finally, Fig. 10 depicts the optimal power schedules of battery (dis)charging amount $P_{b,t}^*$ and the corresponding state of charge C_t^*. The structure revealed in Remark 6 is clearly observed. That is, there is a relatively large amount of battery discharging ($P_{b,t}^* < 0$) when the corresponding price is high (time slots 4 and 5), and the amount of stored energy C_t^*

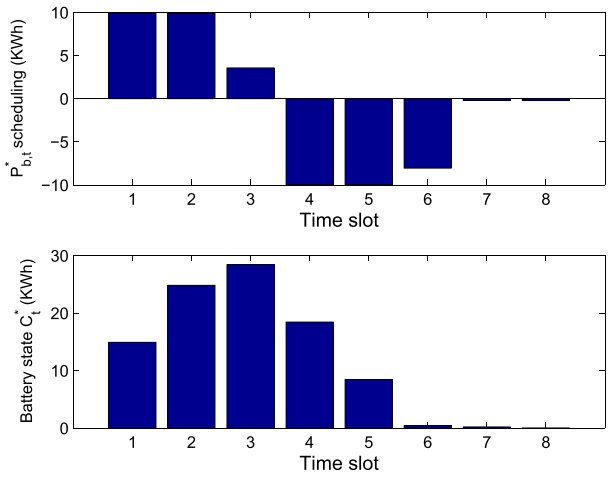

Fig. 10. Optimal power schedules of $P^*_{b,t}$ and C^*_t ($K = 10$, $N_t = 2$).

decreases accordingly. Note that both $P^*_{b,t}$ and C^*_t never exceed their lower and upper limits [cf. Table I].

VI. Conclusions

For a smart-grid powered MIMO BC transmitter with energy harvesting units, robust ahead-of-time optimal resource allocation strategies were proposed to maximize the achievable sum-rate, subject to the worst-case transaction cost. Leveraging practical models and the notion of uplink-dowlink duality, the resource management task was formulated as a convex problem. A low-complexity solver with guaranteed convergence was developed based on the dual decomposition and the proximal bundle method.

Supported by major programs, the smart-grid industry is growing very fast, covering large cities and expanded areas, which is an effective solution for energy-efficient wireless transmission and green communications. As a result, the integration of smart-grid technology into system designs offers a promising solution, which facilitates the development of smart homes, smart parking, and smart transportation. The proposed models and approaches clearly pave a way to advancing study and further research on dynamic operations of these smart systems that will be pursued in our future work.

References

[1] T. M. Cover and J. A. Thomas, *Elements of Information Theory*, 2nd ed. Hoboken, NJ, USA: Wiley, 2006.

[2] L. Li and A. J. Goldsmith, "Capacity and optimal resource allocation for fading broadcast channels—Part I: Ergodic capacity," *IEEE Trans. Inf. Theory*, vol. 47, no. 3, pp. 1083–1102, Mar. 2001.

[3] H. Weingarten, Y. Steinberg, and S. Shamai (Shitz), "The capacity region of the Gaussian multiple-input multiple-output broadcast channel," *IEEE Trans. Inf. Theory*, vol. 52, no. 9, pp. 3936–3964, Sep. 2006.

[4] Y. Zhang, N. Gatsis, and G. B. Giannakis, "Robust energy management for microgrids with high-penetration renewables," *IEEE Trans. Sustainable Energy*, vol. 4, no. 4, pp. 944–953, Oct. 2013.

[5] X. Liu and W. Xu, "Economic load dispatch constrained by wind power availability: A here-and-now approach," *IEEE Trans. Sustainable Energy*, vol. 1, no. 1, pp. 2–9, Apr. 2010.

[6] X. Guan, Z. Xu, and Q.-S. Jia, "Energy-efficient buildings facilitated by microgrid," *IEEE Trans. Smart Grid*, vol. 1, no. 3, pp. 243–252, Dec. 2010.

[7] G. B. Giannakis, V. Kekatos, N. Gatsis, S.-J. Kim, H. Zhu, and B. F. Wollenberg, "Monitoring and optimization for power grids: A signal processing perspective," *IEEE Signal Process. Mag.*, vol. 30, no. 5, pp. 107–128, Sep. 2013.

[8] M. A. Antepli, E. Uysal-Biyikoglu, and H. Erkal, "Optimal packet scheduling on an energy harvesting broadcast link," *IEEE J. Sel. Areas Commun.*, vol. 29, no. 8, pp. 1721–1731, Sep. 2011.

[9] J. Yang, O. Ozel, and S. Ulukus, "Broadcasting with an energy harvesting rechargeable transmitter," *IEEE Trans. Wireless Commun.*, vol. 11, no. 2, pp. 571–583, Feb. 2012.

[10] O. Ozel, J. Yang, and S. Ulukus, "Optimal broadcast scheduling for an energy harvesting rechargeable transmitter with a finite capacity battery," *IEEE Trans. Wireless Commun.*, vol. 11, no. 6, pp. 2193–2203, Jun. 2012.

[11] X. Wang, Z. Nan, and T. Chen, "Optimal MIMO broadcasting for energy harvesting transmitter with non-ideal circuit power consumption," *IEEE Trans. Wireless Commun.*, vol. 14, no. 5, pp. 2500–2512, May 2015.

[12] S. Bu, F. R. Yu, Y. Cai, and X. P. Liu, "When the smart grid meets energy-efficient communications: Green wireless cellular networks powered by the smart grid," *IEEE Trans. Wireless Commun.*, vol. 11, no. 8, pp. 3014–3024, Aug. 2012.

[13] J. Xu and R. Zhang, "CoMP meets smart grid: A new communication and energy cooperation paradigm," *IEEE Trans. Veh. Technol.*, vol. 64, no. 6, pp. 2476–2488, Jun. 2015.

[14] D. Niyato, X. Lu, and P. Wang, "Adaptive power management for wireless base stations in a smart grid environment," *IEEE Wireless Commun.*, vol. 19, no. 6, pp. 44–51, Dec. 2012.

[15] J. Xu and R. Zhang, "Cooperative energy trading in CoMP systems powered by smart grids," *IEEE Trans. Veh. Technol.*, vol. 65, no. 4, pp. 2142–2153, Apr. 2015. [Online]. Available: http://arxiv.org/pdf/1403.5735v2.pdf

[16] T. Han and N. Ansari, "Powering mobile networks with green energy," *IEEE Wireless Commun.*, vol. 21, no. 1, pp. 90–96, Feb. 2014.

[17] Y.-K. Chia, S. Sun, and R. Zhang, "Energy cooperation in cellular networks with renewable powered base stations," *IEEE Trans. Wireless Commun.*, vol. 13, no. 12, pp. 6996–7010, Dec. 2014.

[18] J. Xu, L. Duan, and R. Zhang, "Cost-aware green cellular networks with energy and communication cooperation," *IEEE Commun. Mag.*, vol. 53, no. 5, pp. 257–263, May 2015.

[19] J. Leithon, T. J. Lim, and S. Sun, "Energy exchange among base stations in a cellular network through the smart grid," in *Proc. IEEE ICC*, Jun. 2014, pp. 4036–4041.

[20] X. Wang, Y. Zhang, G. B. Giannakis, and S. Hu, "Robust smart-grid-powered cooperative multipoint systems," *IEEE Trans. Wireless Commun.*, vol. 14, no. 11, pp. 6188–6199, Nov. 2015.

[21] M. H. M. Costa, "Writing on dirty paper," *IEEE Trans. Inf. Theory*, vol. 29, no. 3, pp. 439–441, May 1983.

[22] D. Bertsimas, D. B. Brown, and C. Caramanis, "Theory and applications of robust optimization," *SIAM Rev.*, vol. 53, no. 3, pp. 464–501, Aug. 2011.

[23] K. Tutuncuoglu, A. Yener, and S. Ulukus, "Optimum policies for an energy harvesting transmitter under energy storage losses," *IEEE J. Sel. Areas Commun.*, vol. 33, no. 3, pp. 467–481, Mar. 2015.

[24] T. Li and M. Dong, "Real-time energy storage management with renewable integration: Finite-time horizon approach," *IEEE J. Sel. Areas Commun.*, vol. 33, no. 12, pp. 2524–2539, Dec. 2015.

[25] S. Boyd and L. Vandenberghe, *Convex Optimization*. Cambridge, U.K.: Cambridge Univ. Press, 2004.

[26] N. Jindal, S. Vishwanath, and A. Goldsmith, "On the duality of Gaussian multiple-access and broadcast channels," *IEEE Trans. Inf. Theory*, vol. 50, no. 5, pp. 768–783, May 2004.

[27] D. P. Bertsekas, *Convex Optimization Theory*. Belmont, MA, USA: Athena Scientific, 2009.

[28] P. Youssef-Massaad, L. Zheng, and M. Medard, "Bursty transmission and glue pouring: On wireless channels with overhead costs," *IEEE Trans. Wireless Commun.*, vol. 7, no. 12, pp. 5188–5194, Dec. 2008.

[29] J. Xu and R. Zhang, "Throughput optimal policies for energy harvesting wireless transmitters with non-ideal circuit power," *IEEE J. Sel. Areas Commun.*, vol. 32, no. 2, pp. 322–332, Feb. 2014.

[30] *CVX: MATLAB Software for Disciplined Convex Programming, Version 2.1*, Sep. 2012. [Online]. Available: http://cvxr.com/cvx

[31] MOSEK ApS. (2014). [Online]. Available: http://www.mosek.com/

[32] J. F. Sturm, "Using SeDuMi 1.02, a MATLAB toolbox for optimization over symmetric cones," *Optim. Methods Softw.*, vol. 11, nos. 1–4, pp. 625–633, 1999.
[33] A. Goldsmith, *Wireless Communications*. Cambridge, U.K.: Cambridge Univ. Press, 2005.

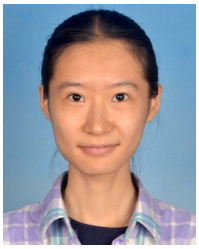

Shuyan Hu received the B.Eng. degree in electrical engineering from Tongji University, Shanghai, China, in 2014. She is currently pursuing the Ph.D. degree with the Department of Communication Science and Engineering, Fudan University, China. Her research interests include wireless resource allocation, smart grid, and green communications.

Yu Zhang (M'16) received the B.Eng. (Hons.) degree from the Wuhan University of Technology, Wuhan, China, in 2006, the M.Sc. (Hons.) degree from Shanghai Jiao Tong University, Shanghai, China, in 2010, and the Ph.D. degree from the University of Minnesota, Minneapolis, MN, USA, in 2015, all in electrical engineering.

He was a Post-Doctoral Associate with the Department of Electrical and Computer Engineering, University of Minnesota. He is currently a Post-Doctoral Scholar with the Department of Industrial Engineering and Operations Research, University of California, Berkeley, Berkeley, CA, USA. His research interests span the areas of smart power grids, optimization theory, machine learning, and wireless communications. His current research focuses on distributed energy management with renewables, and energy data analytics. He received the Huawei Scholarship and the Infineon Scholarship from Shanghai Jiao Tong University (2009), the ECE Department Fellowship from the University of Minnesota (2010), and the Student Travel Awards from SIAM and the IEEE Signal Processing Society (2014).

Xin Wang (SM'09) received the B.Sc. and M.Sc. degrees from Fudan University, Shanghai, China, in 1997 and 2000, respectively, and the Ph.D. degree from Auburn University, Auburn, AL, USA, in 2004, all in electrical engineering.

From September 2004 to August 2006, he was a Postdoctoral Research Associate with the Department of Electrical and Computer Engineering, University of Minnesota, Minneapolis, MN, USA. In August 2006, he joined the Department of Computer and Electrical Engineering and Computer Science, Florida Atlantic University, Boca Raton, FL, USA, where he is an Associate Professor (on leave). He is currently a Distinguished Professor with the Department of Communication Science and Engineering, Fudan University. His research interests include stochastic network optimization, energy-efficient communications, cross-layer design, and signal processing for communications. He served as an Associate Editor for the IEEE SIGNAL PROCESSING LETTERS. He currently serves as an Associate Editor for the IEEE TRANSACTIONS ON SIGNAL PROCESSING and as an Editor for the IEEE TRANSACTIONS ON VEHICULAR TECHNOLOGY.

Georgios B. Giannakis (F'97) received the Diploma degree in electrical engineering from the National Technical University of Athens, Greece, in 1981, the M.Sc. degree in electrical engineering, in 1983, the M.Sc. degree in mathematics, in 1986, and the Ph.D. degree in electrical engineering, in 1986. From 1982 to 1986, he was with the University of Southern California. Since 1999, he has been a Professor with the University of Minnesota, where he currently holds an ADC Chair in Wireless Telecommunications with the ECE Department, and serves as the Director of the Digital Technology Center.

His general interests span the areas of communications, networking, and statistical signal processing, in which he has authored more than 390 journal papers, 660 conference papers, 25 book chapters, 2 edited books, and 2 research monographs (h-index of 117). His current research focuses on learning from big data, wireless cognitive radios, and network science with applications to social, brain, and power networks with renewables. He holds 25 patents issued. He is a fellow of EURASIP, and has served the IEEE in a number of positions, including that of a Distinguished Lecturer of the IEEE Signal Processing (SP) Society. He is a co-recipient of eight best paper awards from the IEEE SP and Communications Societies, including the G. Marconi Prize Paper Award in Wireless Communications. He received Technical Achievement Awards from the SP Society (2000) and from EURASIP (2005), a Young Faculty Teaching Award, the G. W. Taylor Award for Distinguished Research from the University of Minnesota, and the IEEE Fourier Technical Field Award (2015).